FEM simulation of a sono-reactor accounting for vibrations of the boundaries.

O. Louisnard [a,1], J. Gonzalez Garcia [b], I. Tudela [b], J. Klima [c], V. Saez [b], Y. Vargas [d],

[a] *Laboratoire de Génie des Procédés des Solides Divisés, UMR CNRS 2392, École des Mines d'Albi-Carmaux, Campus Jarlard, 81013 Albi Cedex 09, France*

[b] *Departamento de Química Física e Instituto Universitario de Electroquímica, Universidad de Alicante, Spain.*

[c] *J. Herovsky Institute of Physical Chemistry Academy of Sciences of the Czech Republic, 18223 Prague 8, Czech Republic.*

[d] *Laboratorio de Ultrasonidos, USACH, Casilia 307, Santiago 2, Chile*

Abstract

The chemical effects of acoustic cavitation are obtained in sono-reactors built-up from a vessel and an ultrasonic source. In this paper, simulations of an existing sono-reactor are carried out, using a linear acoustics model, accounting for the vibrations of the solid walls. The available frequency range of the generator (19 kHz-21 kHz) is systematically scanned. Global quantities are plotted as a function of frequency in order to obtain response curves, exhibiting several resonance peaks. The attenuation coefficient of the wave is taken as a variable parameter, in absence of the precise knowledge of the bubble size distribution, and its influence is studied. The concepts of acoustic energy, intensity and active power are recalled, along with the general balance equation for acoustic energy. The latter is used as a convergence check of the simulations. Finally, it is shown that the interface between the liquid and the solid walls cannot be correctly represented by the simple approximations of either infinitely soft, or infinitely hard boundaries. Moreover, the liquid-solid coupling allows the cooling jacket to receive a noticeable part of the input power, although it is not in direct contact with the sonotrode. It may therefore undergo cavitation and this feature opens the perspective to design sono-reactors which avoid direct contact between the working liquid and the sonotrode.

Key words: finite elements, ultrasound, linear acoustics, bubble, cavitation,
PACS: 47.57.ef
PACS: 47.55.dd
PACS: 68.55.Ac

1. Introduction

When a liquid is irradiated by a high-power ultrasonic wave, numerous radially oscillating micron-sized bubbles appear. The phenomenon is known as acoustic cavitation [1, 2]. The strong collapse, following the explosive expansion of these bubbles, induces extreme conditions inside or near the bubbles, which are responsible for a specific chemistry, known as sonochemistry [3].

Various experimental devices can be used to produce this phenomenon. The most common one is a horn transducer, diving in the liquid and creating large acoustic pressure in its vicinity. Other systems involve a transducer with larger emitting area, from the bottom (sometimes referred as "cup-horn reactors"), or various transducers sticked to plane walls, the latter system being commonly known as ultrasonic bath.

Email address: louisnar@enstimac.fr (O. Louisnard).
[1] Corresponding author

It is generally accepted that horn transducers, as they are very thin, emit more or less a spherical wave, thus decaying rapidly as the distance from the tip increases. Besides, transducers with larger area rather create standing waves, by reflexion of the emitted waves on the vessel wall. This difference has indeed consequences on the self-organization of bubbles in an astonishing variety of spatial structures [4]. Horn transducer are known to produce an intense cavitation field near its tip, while the standing waves created by large-area transducer can attract bubbles at or near antinodes, possibly far from the emitting surface.

However, a clear distinction between the two configurations is not fully justified by theoretical acoustics. A horn-type transducer emitting in a thin vessel may also create standing waves, whereby a large area transducer emitting in a giant vessel would not. The relevant parameter is not only the ratio of the transducer size to the vessel dimensions, but also the ratio of the vessel dimensions to the acoustic wavelength. In fact, any closed acoustic system presents normal vibration modes at definite frequencies, and resonates when excited at these frequencies. Some available commercial systems exploit this property, and adjust automatically the working frequency (in a reasonable range), in order to excite a normal mode of the vessel. One of the motivation of this paper is to assess the existence of these resonance modes by simulation.

The question arises if such resonant behaviors can be reasonably predicted by linear acoustics. At first sight, it might sound doubtful, since high-amplitude waves are subject to nonlinear phenomena, even in homogeneous liquids. Moreover, the presence of cavitation bubbles modifies the acoustic properties of the effective medium, decreasing the effective sound velocity, and introducing dispersion and nonlinear phenomena [5, 6, 7]. However, in most cases, the bubbles are concentrated in relatively small regions of the liquid, and one could expect that linear acoustics may at least give a qualitative idea of the acoustic field and the approximate location of the various resonance frequencies, in the first step of the design of a sono-reactor.

Even in the restricted frame of linear acoustics, there remains the problem of the suitable boundary conditions. Precedent studies generally treat the vessel boundaries either as infinitely rigid walls [8], or infinitely soft [9]. Solid boundaries may in fact be thin enough to vibrate and deform, and these effects must be considered, if one seeks precisely the resonant modes of the system. Simulations of a sono-reactor accounting for vibrations of the vessel wall have been recently published [10], and show the effect of the vessel wall thickness in a rectangular cell for two frequencies, 100 kHz and 140 kHz. Here we present the response of an experimental sono-reactor, including a cooling jacket, excited by a cup-horn type transducer. The simulation presented hereafter account for the vibration of the boundaries, and possible transmission of sound into the cooling jacket. The frequency is systematically varied in the range available for the generator used, the resonances of the whole structure are sought and characterized by calculating several global quantities as functions of frequency.

Besides, we recall the concepts of acoustic energy density, acoustic intensity and active power, which are sometimes confusingly used. It is first recalled, on rigorous arguments, that if no wave escapes from the sonoreactor, the active power is nothing else than the power dissipated in the liquid. The latter can be estimated by recording the initial temperature increase, which forms the basis of the calorimetric method [11].

2. Equations of the problem

2.1. *Linear acoustics in the liquid*

The linear propagation of an acoustic wave is described by the linearization of the Euler equations [12]:

$$\frac{1}{\rho_l c_l^2}\frac{\partial p}{\partial t} + \boldsymbol{\nabla}.\mathbf{v} = 0, \tag{1}$$

$$\rho_l \frac{\partial \mathbf{v}}{\partial t} = -\boldsymbol{\nabla} p, \tag{2}$$

where $\mathbf{v}(\mathbf{x}, t)$ is the liquid velocity field associated to the acoustic wave, $p(\mathbf{x}, t)$ the local acoustic pressure, and ρ_l, c_l are the density and the sound speed of the liquid, respectively.

We assume mono-harmonic waves at angular frequency ω. In what follows, we will use the complex notation

$$p(x, y, z, t) = \tfrac{1}{2}\left[P(x, y, z)e^{i\omega t} + P^*(x, y, z)e^{-i\omega t}\right], \tag{3}$$

$$\mathbf{v}(x, y, z, t) = \tfrac{1}{2}\left[\mathbf{V}(x, y, z)e^{i\omega t} + \mathbf{V}^*(x, y, z)e^{-i\omega t}\right], \tag{4}$$

Equations (1), (2) transform to

$$i\omega P + \rho_l c_l^2 \boldsymbol{\nabla}.\mathbf{V} = 0, \quad (5)$$

$$i\omega \rho_l \mathbf{V} = -\boldsymbol{\nabla} P, \quad (6)$$

and eliminating $\mathbf{V}$ between the two equations yields the well-known Helmholtz equation

$$\nabla^2 P + k_l^2 P = 0, \quad (7)$$

where $k_l = \omega/c_l$ is the wavenumber.

2.2. *Boundary conditions for the liquid*

The free surface in the reactor, if any, is generally represented by an infinitely soft boundary, that is $p = 0$, or $P = 0$ in the case of mono-harmonic waves.

On the radiating surface of the transducer, one generally assumes that the normal displacement is known. This is an over-simplification, and a correct representation would involve the modelization of all parts of the transducer, including the piezoceramics, and an appropriate coupling with the fluid. In a first approach, we will however use this simplification here. Noting U_0 the complex amplitude of the transducer displacement, and using (6), the boundary condition for the fluid reads

$$\boldsymbol{\nabla} P.\mathbf{n} = \rho_l \omega^2 U_0, \quad (8)$$

where $\mathbf{n}$ is the normal pointing outward the liquid.

In past studies, the walls of the vessel enclosing the liquid have been either also considered as infinitely soft ($P = 0$) [9], or infinitely rigid [8]. The latter condition imposes a zero normal velocity, which, for mono-harmonic waves, using (6), translates to $\boldsymbol{\nabla} P.\mathbf{n} = 0$. To relax any of these two simple approximations, the vibration of the solid parts must be properly accounted for.

2.3. *Vibration of the solid*

Neglecting the volumic forces, the vibrations of an elastic solid are given by:

$$\rho_s \frac{\partial^2 \mathbf{u_s}}{\partial t^2} = \boldsymbol{\nabla}.\overline{\overline{\boldsymbol{\sigma}}}, \quad (9)$$

where ρ_s is the solid density. $\mathbf{u_s}(x, y, z, t)$ is the displacement field and $\overline{\overline{\boldsymbol{\sigma}}}$ the elastic stress tensor given by

$$\overline{\overline{\boldsymbol{\sigma}}} = \frac{E\nu}{(1-2\nu)(1+\nu)} (\mathrm{Tr}\overline{\overline{\boldsymbol{\epsilon}}})\, \overline{\overline{\mathbf{I}}} + \frac{E}{1+\nu}\, \overline{\overline{\boldsymbol{\epsilon}}}, \quad (10)$$

where E is the Young modulus, ν the Poisson ratio, $\overline{\overline{\mathbf{I}}}$ the identity tensor, Tr the trace operator, and $\overline{\overline{\boldsymbol{\epsilon}}}$ the strain tensor:

$$\overline{\overline{\boldsymbol{\epsilon}}} = \frac{1}{2}\left[\overline{\overline{\nabla}}\mathbf{u_s} + {}^T\overline{\overline{\nabla}}\mathbf{u_s}\right]. \quad (11)$$

For mono-harmonic vibrations, the displacement field is set as

$$\mathbf{u_s}(x, y, z, t) = \tfrac{1}{2}\left[\mathbf{U_s}(x, y, z)e^{i\omega t} + \mathbf{U_s}^*(x, y, z)e^{-i\omega t}\right], \quad (12)$$

so that Eq. (9) becomes

$$-\rho_s \omega^2 \mathbf{U_s} = \boldsymbol{\nabla}.\overline{\overline{\boldsymbol{\Sigma}}}, \quad (13)$$

where

$$\overline{\overline{\boldsymbol{\Sigma}}} = \frac{E\nu}{(1-2\nu)(1+\nu)} (\mathrm{Tr}\overline{\overline{\boldsymbol{\mathcal{E}}}})\, \overline{\overline{\mathbf{I}}} + \frac{E}{1+\nu}\, \overline{\overline{\boldsymbol{\mathcal{E}}}}, \quad (14)$$

$$\overline{\overline{\boldsymbol{\mathcal{E}}}} = \frac{1}{2}\left[\overline{\overline{\nabla}}\mathbf{U_s} + {}^T\overline{\overline{\nabla}}\mathbf{u_s}\right]. \quad (15)$$

2.4. *Boundary conditions for the solid*

The boundary conditions for the solid may either prescribe any component of the displacement field, or the components of the stress acting on the surface. On the boundaries in contact with air, the three components of the stress are to be ascribed to zero.

2.5. *Liquid-solid interface conditions*

The coupling between the liquid and solid vibrations are obtained by writing two interface conditions on such surfaces. The first one is a cinematic condition, and just states that the displacement is continuous on each side of the interface, so that the condition

$$\mathbf{v}.\mathbf{n} = \frac{\partial \mathbf{u_s}}{\partial t}.\mathbf{n} \quad (16)$$

must hold, $\mathbf{n}$ being the normal vector pointing outward the liquid. For mono-harmonic waves, derivating this relation and using (6) yields

$$\boldsymbol{\nabla} P.\mathbf{n} = \rho_l \omega^2 \mathbf{U_s}.\mathbf{n}, \quad (17)$$

which is used as a boundary condition for linear acoustics in the liquid.

The second condition is a dynamic one, and states that the normal force per unit area exerted on the solid boundary in contact with the liquid is just the pressure of the liquid, which reads

$$\overline{\overline{\boldsymbol{\Sigma}}}.\mathbf{n} = -P\mathbf{n}. \quad (18)$$

This continuity equation is used as a boundary conditions for equation (9) governing the vibration of the solid.

3. Energy consideration

3.1. *Conservation of acoustic energy*

If attenuation due to energy absorption is ignored, the equation of acoustic energy conservation can be readily deduced from Eqs. (1), (2), and reads [12]

$$\frac{d}{dt}\iiint_V e_a \,\mathrm{d}V = \iint_S -\mathbf{I}.\mathbf{n}\,\mathrm{d}S, \tag{19}$$

where V is an arbitrary volume of fluid, S its boundary. The quantity

$$e_a = \frac{1}{2}\rho_l \mathbf{v}^2 + \frac{1}{2}\frac{p^2}{\rho_l c_l^2} \tag{20}$$

is the acoustic energy density (in $\mathrm{W/m^3}$), which is the sum of the kinetic energy and the potential compressional energy of the liquid, and

$$\mathbf{I} = p\mathbf{v} \tag{21}$$

is the acoustic intensity (in $\mathrm{W/m^2}$). Both e_a and $\mathbf{I}$ are local quantities, and it should be recalled that $\mathbf{I}$ is a vector field, which streamlines represent the path followed by acoustic energy. Equation (19) just expresses that the acoustic energy variations in a volume of fluid, results from the difference between the energy flux entering and the one leaving this volume. From a mechanical point of view, this equation is just the consequence of the kinetic energy theorem: the surface integral is the power of external pressure forces on S, the integral of $\frac{1}{2}\rho_l\mathbf{v}^2$ is the total kinetic energy in V, and the volume integral of $\frac{1}{2}p^2/(\rho_l c_l^2)$ is the opposite of the power of internal pressure forces.

3.2. *Active power*

Cavitation experiments are commonly characterized by the acoustic power sent to the liquid through the sonotrode surface. First, we would like to recall that, for periodic waves, non-dissipative linear acoustics predicts a null value for the latter quantity on average over one period, in the case of perfectly reflecting boundaries.

Indeed, the acoustic energy e_a reads, with expressions (3), (4):

$$e_a = \frac{1}{4}\rho_l|\mathbf{V}|^2 + \frac{1}{4}\frac{|P|^2}{\rho_l c_l^2} + \text{oscillating terms}, \tag{22}$$

so that the left-side of Eq. (19) is zero on average over one acoustic period. Besides, using (3), (4), the acoustic intensity $\mathbf{I}$ is found to read

$$\mathbf{I} = \frac{1}{2}\Re\left(P\mathbf{V}^*\right) + \text{oscillating terms}, \tag{23}$$

where $\Re$ denotes the real part of a complex number.

Now, let's consider the case of a sono-reactor excited by the vibrating surface $S_{\text{sonotrode}}$ of a sonotrode, and closed by boundaries $S_{\text{boundaries}}$, of unspecified type for now. When averaged over one period, the energy conservation equation (19) becomes therefore

$$P_{\text{active}} = P_{\text{bound}} \tag{24}$$

where

$$P_{\text{active}} = \iint_{S_{\text{sonotrode}}} -\frac{1}{2}\Re(P\mathbf{V}^*).\mathbf{n}\,\mathrm{d}S, \tag{25}$$

$$P_{\text{bound}} = \iint_{S_{\text{boundaries}}} \frac{1}{2}\Re(P\mathbf{V}^*).\mathbf{n}\,\mathrm{d}S. \tag{26}$$

Integral (25) is the power entering the liquid through the sonotrode area, and is termed as active power, while (26) is the power lost through the other (passive) boundaries of the liquid. Thus Eq. (24) states that, once the standing wave has built-up, the liquid cannot store more energy on average over one period. All the energy entering the liquid per unit-time is lost by boundaries. When the boundaries do not transmit any wave to the external air, P_{bound} is zero. This is the case for example in the simple cases of infinitely soft ($P = 0$) or infinitely rigid boundaries ($\mathbf{V} = \mathbf{0}$). In the more complex case where $S_{\text{boundaries}}$ is the internal wall of the solid vessel, its external wall being unconstrained, it can be demonstrated that P_{bound} is still zero. Therefore, in all these cases, equation (24) merely states that, without absorption of ultrasonic energy and/or transmission of some energy to an external space, the acoustic power P_{active} transmitted to the liquid by the sonotrode should be zero.

3.3. *Attenuation and energy dissipation*

The latter result sounds paradoxical, but originates from the non-dissipative character of the medium which is implicitly assumed in Eqs. (2). It is therefore meaningless to try to predict the active power transmitted to a reactor with non-dissipative linear acoustics. Dissipation in acoustic waves occurs for various reasons: viscosity of the medium,

diffusion of compressional heat energy at finite rate, and relaxation delay in the case of gases. For linear mono-harmonic wave, this effects can be represented by a complex wavenumber (or sound velocity)

$$k = k_r - i\alpha, \tag{27}$$

where $\alpha > 0$ is the attenuation coefficient, and $k_r = \omega/c_l$. In the case of cavitation, the dissipation occurs at the level of each bubble, and origin from viscous friction, heat diffusion in the bubble, and acoustic radiation [13, 14, 15, 16]. The corresponding sound velocity and attenuation factor of linear acoustic waves in a bubbly liquid can be expressed easily, once the bubbles size-distribution function is known [6]. The latter theory has been used by several authors, but setting an arbitrary Gaussian-shaped distribution of bubble sizes [17, 18, 19]. Moreover, it is well known that, owing to Bjerknes forces, the cavitation bubbles are not homogeneously distributed in the whole liquid, but rather arrange in complex localized structures [4]. Owing to the lack of a theory yielding a physical choice of the attenuation factor, we chose to treat the latter quantity as a variable parameter in the simulations presented hereafter.

It is instructive to see how the energy balance (24) can be generalized to the case of dissipative wave propagation, without detailing the physical origin of dissipation, but knowing the attenuation factor α. It is shown in appendix (A) that the energy balance equation (24) becomes

$$P_{\text{active}} = P_{\text{bound}} + P_{\text{diss}}, \tag{28}$$

where

$$P_{\text{diss}} = \iiint_V \alpha \frac{|P|^2}{\rho_l c_l} \, \mathrm{d}V, \tag{29}$$

and P_{active}, P_{bound} are still given by (25), (26). The integral (29) is positive, and represents the opposite of the mechanical power of the dissipative internal forces. Equation (28) therefore states that the active power entering the medium, either flows out through other boundaries, or is dissipated in the medium. This relation is useful to check the validity of the simulation results.

3.4. *The plane wave hypothesis*

The hypothesis of plane traveling waves (PTW) for a vibrating boundary emitting in a liquid allows to obtain simple expressions of velocity, acoustic pressure, and therefore of the active power sent through the emitter

$$P_{\text{active}}^{\text{PTW}} = \frac{1}{2}\frac{|P_0|^2}{\rho_l c_l} S_{\text{sonotrode}} = \frac{1}{2}\rho_l c_l |\mathbf{V}_0|^2 S_{\text{sonotrode}}, \tag{30}$$

where $|P_0|$ and $|\mathbf{V}_0|$ are the peak values of the acoustic pressure and fluid velocity, respectively, on the sonotrode's surface. This expression would have the advantage to deduce directly the active power to the amplitude of the emitter. We will show however that this approximation, for a closed geometry where standing wave are expected, definitely yields unrealistic results.

4. The problem solved

4.1. *Experimental configuration studied*

The experimental setup simulated is represented in Figure 1. Since it presents axial symmetry, only one half of a cut plane is represented. The sonotrode emits from below in a liquid in contact with air on its upper surface, and limited laterally by thin glass walls. The sono-reactor also presents a cooling jacket to maintain the temperature constant along an experiment. A Teflon ring prevents the fluid to leak downward and maintains the whole setup. The liquid in the reactor and in the cooling jacket is water with properties $\rho_l = 1000$ kg.m^{-3} and $c_l = 1500$ m.s^{-1}. The elastic properties are $E = 73$ GPa, $\nu = 0.17$ for glass and $E = 0.5$ GPa, $\nu = 0.46$ for Teflon. The liquid height is fixed to $h = 72$ mm, counted from the vibrating surface of the sonotrode. The latter is assumed to vibrate vertically with an amplitude of 10^{-6} m.

The sonotrode is constituted internally from a sandwich transducer excited by a variable frequency generator (20 kHz - 100 W, Undatim) [8]. The system is able to scan the emission frequency between 19 kHz and 21 kHz, and records the frequency for which the electrical impedance on the transducer terminals is minimal. This allows experimentally to work at a frequency at which the system presents a resonance, if any.

4.2. *Simulation strategy*

The problem defined in section 2 is solved with the COMSOL software, varying the frequency by small steps in the range [19 kHz,21 kHz]. Scalar quantities representative of the global vibration of the system are computed and plotted as functions of frequency,

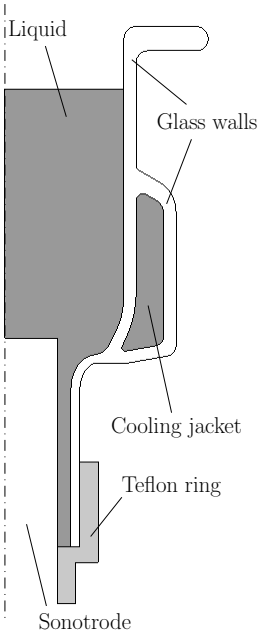

Fig. 1. Geometry studied. Only one-half of the reactor is drawn.

in order to get a clear picture of the system's resonances.

The computed quantities can be chosen among the following:

– the average acoustic energy stored in the liquid:

$$E_{a,l} = \iiint_V \left(\frac{1}{4}\rho_l \left|\mathbf{V}\right|^2 + \frac{1}{4}\frac{\left|P\right|^2}{\rho_l c_l^2} \right) \mathrm{d}V, \quad (31)$$

– the average acoustic energy stored in the solid walls, either Teflon and glass. The latter quantity can be written as

$$E_{a,s} = \iiint_{V_{\text{walls}}} \left[\frac{1}{4}\rho_s \omega^2 \left|\mathbf{U_s}\right|^2 + \frac{1}{2}\Re(\overline{\overline{\mathbf{\Sigma}}} : \overline{\overline{\boldsymbol{\mathcal{E}}}}^{\,*}) \right] \mathrm{d}V, \quad (32)$$

where the first term represents the kinetic energy density, and the second is the deformation energy density of the solid.

– the average acoustic pressure in the liquid:

$$P_{\text{av}} = \frac{1}{V} \iiint_V \left|P\right| \mathrm{d}V, \quad (33)$$

– the power dissipated in the liquid

$$P_{\text{diss}} = \iiint_V \alpha \frac{\left|P\right|^2}{\rho_l c_l} \mathrm{d}V, \quad (34)$$

where V may be the volume of the working liquid, of the cooling liquid in the jacket, or the sum of both,

– the active power entering the liquid through the sonotrode

$$P_{\text{active}} = \iint_{S_{\text{sonotrode}}} -\frac{1}{2}\Re(P\mathbf{V}^*).\mathbf{n}\,\mathrm{d}S. \quad (35)$$

As seen above, from Eq. (28), the two quantities P_{diss} and P_{active} should be the equal, which is checked for each simulation as a convergence test. Besides, a mesh convergence study has been performed.

5. Results and discussion.

5.1. *Response curves*

Figure 2 displays the mean acoustic pressure in the reactor as a function of frequency, with zero attenuation, in the following case: cooling jacket filled with water (thick solid line), cooling jacket empty (thin solid line), internal walls considered as hard boundaries (dashed line), or as soft boundaries (dash-dotted line). In the two latter cases, the vibration of the glass and Teflon walls are not accounted for, and it is clearly seen that the response curves differ significantly from the ones obtained by properly taking into account the walls vibration.

The peaks observed in the response curve correspond to global resonances of the whole mechanical system formed by the liquid coupled with the solid walls. In absence of dissipation, the amplitude of these peaks should be infinite, which would traduce an infinite accumulation of acoustic energy in the system. This does not appear on Fig. 2 owing to the discretization of the frequencies. It is interesting to note that the response curves, with the cooling jacket respectively filled and empty, present approximately the same set of peaks, shifted in frequency, except for peak II which is specific to the filled cooling jacket, which demonstrates the strong influence of the operating conditions on the response of the system.

We now focus on the case where the cooling jacket is filled with water (Fig. 2, thick solid line). Figure 3 displays the instantaneous acoustic pressure $p(r, z, t)$ at $\omega t = 0$, $\pi/2$ and π near peak IV ($f = 20610$ Hz). White zones correspond to large positive acoustic pressures, while black ones correspond to large negative acoustic pressures. Both black or white regions therefore indicate the loci of pressure antinodes, while gray ones represent pressure nodes.

The deformed boundary (magnified) is also displayed, in order to illustrate the coupling between

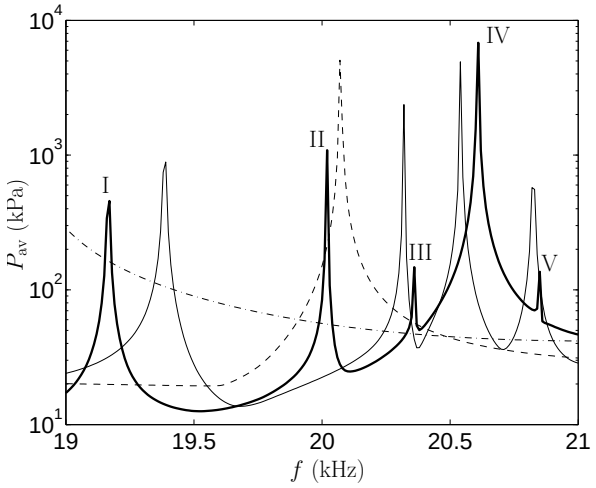

Fig. 2. Response curves of the sono-reactor. Thin solid line: cooling jacket empty. Thick solid line: cooling jacket filled. Dashed line: solid boundaries considered infinitely rigid. Dash-dotted line: solid boundaries considered as infinitely soft.

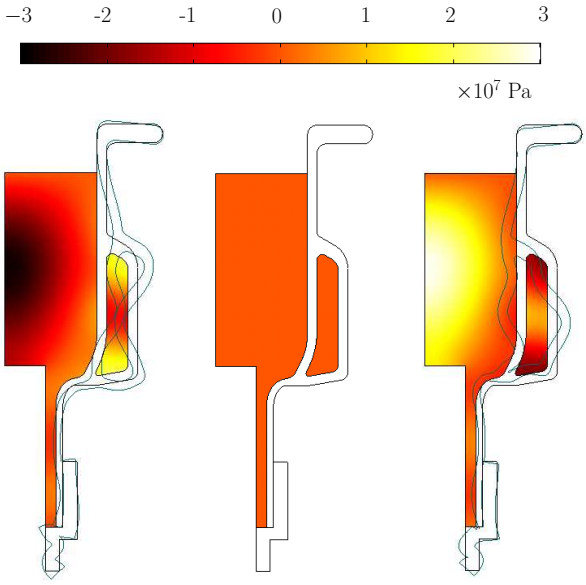

Fig. 3. Pressure field $p(r, z, t)$ and wall deformation near peak IV ($f = 20610$ Hz) at times $\omega t = 0$, $\omega t = \pi/2$, $\omega t = \pi$. The wall displacement is magnified 100 times.

the vibrations of the fluid and the solid. The latter effect is remarkable in the breathing behavior of the cooling jacket: for $\omega t = 0$, the negative pressure sucks the glass walls, while the positive pressure repels them for $\omega t = \pi$. Similar behaviors have been evidenced in Ref. [10]. The uniform gray color observed for $\omega t = \pi/2$ corresponds to the phase at which the acoustic pressure crosses zero uniformly in the reactor. At this time, the velocity field takes its maximal value both in the liquid and the solid. This behavior is well-known for standing waves, and it can be shown that in absence of dissipation, pressure and velocity are indeed in phase quadrature, so that, from Eq. (23), the acoustic intensity is zero everywhere. It is thus retrieved that the acoustic power is zero, in absence of dissipation.

And interesting feature observable in Fig. 3 is the presence of a pressure antinode inside the cooling jacket, which suggests that cavitation can appear in a cavity insulated from the sonotrode by a glass wall. This is indeed often observed experimentally, and we emphasize that this effect demonstrates clearly the role of the wall vibrations, and the need of their proper representation in reliable simulations.

Another important point is that, at this resonant frequency, the pressure antinode appears far from the emitter. The emitting area of sonotrodes are known to suffer erosion, because cavitation near solid surfaces produces liquid jets and shock waves, responsible for the destructive effects [20]. The present simulation suggests that, exciting the sono-reactor near a resonant frequency could help to avoid this problem. This has been mentioned in precedent studies, and confirmed experimentally [9].

To pursue this issue, it is instructive to examine the pressure field obtained far from a resonance, for example at $f = 19500$ Hz (see the response curves in Fig. 2). Figure 4 shows that in this case, the pressure antinode is located near the emitter, and the pressure amplitude rapidly decreases with the distance from the emitter. This behavior is commonly observed experimentally, and the decay of acoustic pressure far form the sonotrode is often attributed to attenuation of the wave by cavitation bubbles. Since no attenuation was introduced in the simulation of Fig. 4, the present result demonstrates that this is not necessary the case. The pressure field observed rather indicates that the sonotrode mainly emits a diverging spherical wave, which has strongly decayed in amplitude when it reaches the boundaries. Nevertheless, as seen in Fig. 4 it is still strong enough to excite the breathing mode of the cooling jacket.

5.2. *Effect of attenuation*

The orders of magnitude of pressure indicated in Fig. 2, 3, 4 may sound unrealistic, especially near resonance. This is expected since no attenuation was introduced in the simulations. We therefore repeated

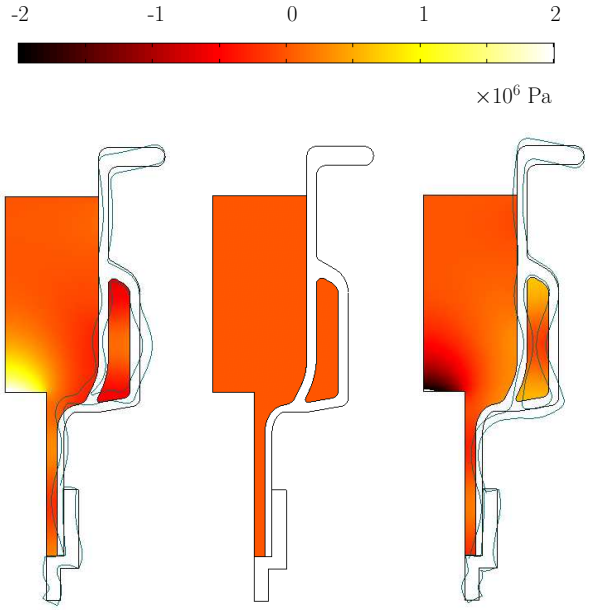

Fig. 4. Pressure field $p(r, z, t)$ and wall deformation for $f = 19500$ Hz at times $\omega t = 0$, $\omega t = \pi/2$, $\omega t = \pi$. The wall displacement is magnified 20000 times.

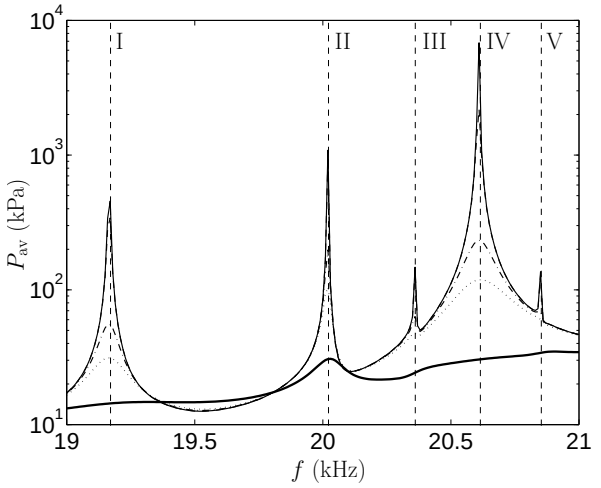

Fig. 5. Mean acoustic pressure peak amplitude P_{av} vs. frequency, for various attenuation coefficients. Thin solid line: $\alpha = 0$. Dashed line: $\alpha = 0.05$. Dash-dotted line: $\alpha = 0.5$. Dotted line: $\alpha = 1$. Thick solid line: $\alpha = 5$.

the computations for different values of the attenuation coefficient: $\alpha = 0.05, 05, 1$ and 5 m^{-1}. Figure 5 displays the response curves obtained. Far from resonances, the effect is weak, except for the largest value $\alpha = 5$ m^{-1} (thick solid line). Near resonances, the mean acoustic pressure decreases strongly with attenuation, and some resonance peaks even disappear when increasing attenuation, especially peaks III and V.

Attenuation not only influences the amplitude of the acoustic field, but also the structure of the pressure field. This is evidenced in Figure 6, which represents the spatial distribution of the peak pressure amplitude $|P|$ in the reactor, near resonance peak IV, and for increasing α (from left to right). A first structural change occurs between the first two fields, as attested by the contour lines and the shape of the glass walls. However, in the first three cases, the pressure antinode remains in the middle of the reactor. The shapes of the field and boundaries deformation are identical for $\alpha = 0.5$ and 1. For the highest attenuation coefficient, the pressure antinode comes back near the transducer, as it would far from resonances. This feature therefore chastens the above remark about the utilization of resonances to keep the pressure antinode away from the tip of the sonotrode.

5.3. *Active and dissipated power*

As seen from Eq. (28), the active power is also the power dissipated in the liquid, and should therefore vary with the attenuation coefficient α. This is illustrated in figure 7. Near resonances, the active power drastically decreases as the attenuation coefficient is increased. Conversely, far from resonances, the opposite occurs: the higher the attenuation, the higher the active power. The latter behavior may sound non-intuitive, but it can be seen from equation (29) that the dissipated power indeed increases both with the attenuation coefficient and the square of the acoustic pressure amplitude. Far from resonance the amplitude of the sound field varies slightly with attenuation coefficient, so that the variation of P_{diss} is mainly governed by the variation of α. Conversely, near resonance, the pressure amplitude at the antinode increases drastically, and a slight increase in the attenuation coefficient yields a huge increase of energy dissipated near the antinode, thus increasing the active power. In mode physical words, near resonance, the liquid stores more acoustic energy, so that it can dissipate more.

Besides, the thick solid line in Fig. 7 represents the active power that would be calculated in the case of a plane traveling wave by Eq. (30). It can be seen that the value obtained is far from being realistic for the whole range of frequencies and attenuation coefficients considered, and mainly overestimates the active power. This could be expected,

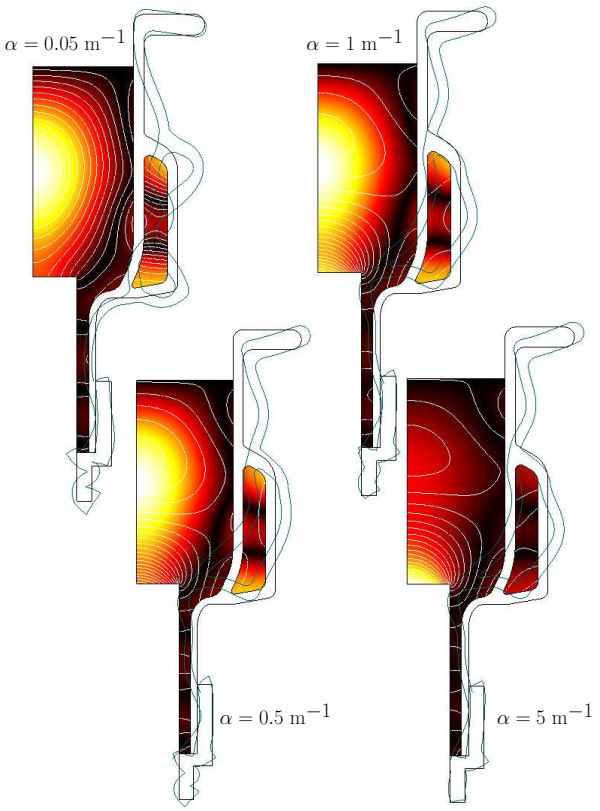

Fig. 6. Repartition of the peak acoustic pressure $|P|$ in the reactor for $f = 20610$ Hz and increasing attenuation coefficients. The color scales are different for each image.

since on one hand, the geometry clearly cannot favor plane waves, and on the other hand, the presence of reflecting boundaries anyway prohibits the existence of traveling waves.

Finally, figure 8 displays the ratio of the dissipated power in the cooling liquid to the total active power sent by the sonotrode for $\alpha = 0.05$, 1 and 5. It is seen that in the whole range of frequencies, a noticeable part of the energy enters the cooling jacket and is dissipated inside. Besides, it can be seen that the curves in Fig. 8 cross some resonances (I and IV) without varying noticeably. This is an indication that such resonances are the result of a collaborative coupling between the working liquid and the liquid in the cooling jacket.

5.4. *Vibration of the solid*

It is instructive to compare the acoustic energy stored in the glass walls to the one stored in the liquid. Figure 9 displays the ratio of both quantities, calculated respectively from Eqs. (31) and (32). It

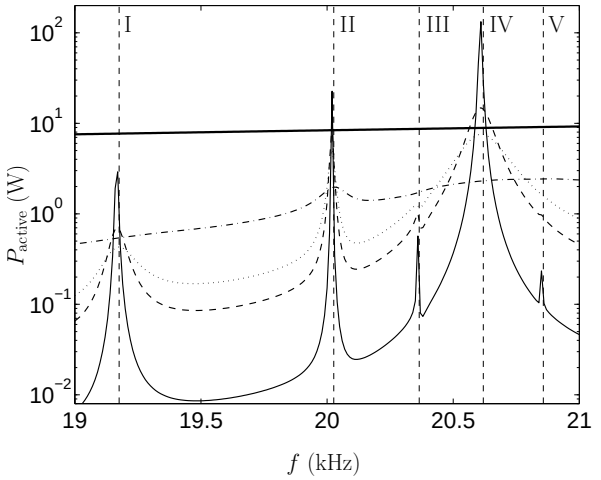

Fig. 7. Active power sent through the emitter, for various attenuation coefficients. Solid line: $\alpha = 0.05$. Dashed line: $\alpha = 0.5$. Dotted line: $\alpha = 1$. Dash-dotted line: $\alpha = 5$. The thick line represents the active power calculated under the hypothesis of a plane traveling wave Eq (30).

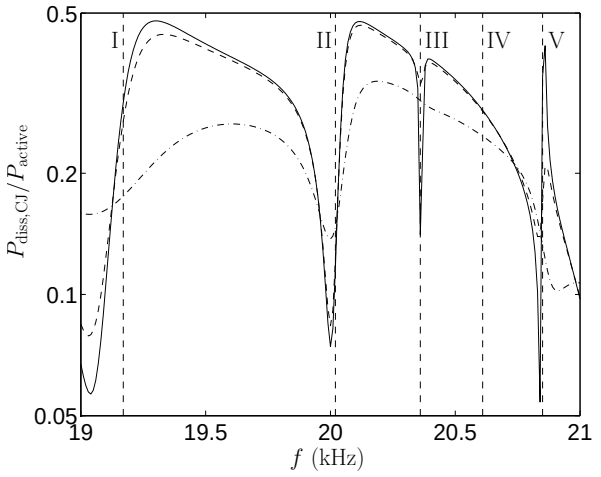

Fig. 8. Ratio of the power dissipated in the cooling jacket to the active power sent by the sonotrode. Solid line: $\alpha = 0.05$. Dashed line: $\alpha = 1$. Dash-dotted line: $\alpha = 5$.

can be seen they are of the same order of magnitude for any frequency and attenuation coefficient, which demonstrates again that the role of the walls deformation.

An interesting feature appears on Fig. 9: some resonance peaks are still visible on the curves: peak IV completely disappears, which means that this resonance is mainly governed by the liquid. Conversely peak V is considerably magnified, which attests that it is rather governed by the solid. Indeed, a calculation of the normal modes of vibration of the solid walls alone, exhibits a resonance frequency

near 20800 Hz. Peaks I and II are smoothed but still visible, and are found to result from a coupling between the working fluid, the cooling fluid and the solid vibrations.

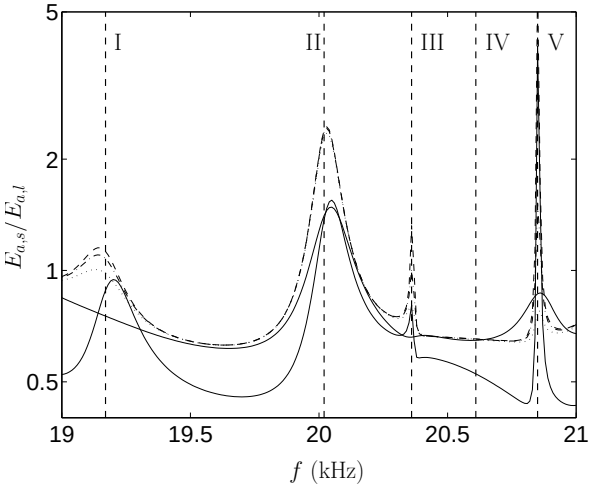

Fig. 9. Ratio of the acoustic energy stored in the glass walls to the acoustic energy stored in the liquid (both the working liquid and the cooling jacket liquid).

5.5. *Sensitivity to liquid properties*

In order to emphasize the influence of the operating conditions on the behavior of the system, Figure 10 compares the response curves obtained when the density of the cooling liquid is decreased to 950 kg.m^{-3}. The five resonance peaks are still visible, but peaks I, IV and V are slightly shifted toward higher frequencies. Thus, even a slight change in density in the cooling jacket, for example produced by a temperature variation of the liquid, can produce a noticeable detuning of the system, if the latter does not lock automatically near a resonance. Besides, it is seen that the location of peaks II and III are not influenced by the properties of the liquid, which demonstrates that the vibrations of the cooling fluid contributes little to these two resonance effects.

6. Conclusion

Simulations of a real sono-reactor have been carried out, taking into account the vibrations of the walls. The frequency was systematically scanned in the range available for the generator used, in order to detect the resonances of the global system.

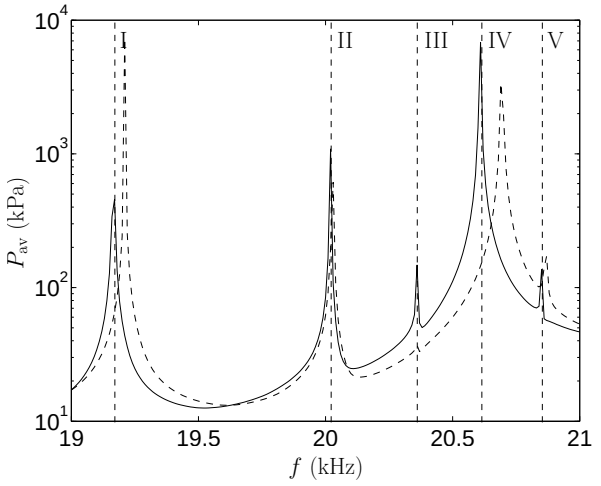

Fig. 10. Response curves obtained for a density of the liquid in the cooling jacket 1000 kg.m^{-3} (solid line) and 950 kg.m^{-3} (dashed line).

It has been shown that the simple hypothesis classically used at the liquid boundaries, either soft or hard wall, definitely yields unrealistic results, and could not anyway predict the sound field in the cooling jacket. Indeed, the vibration of the solid walls induce a significant coupling between the reacting liquid and the cooling liquid. Simulation predicts that a noticeable energy fraction can be transmitted to the liquid in the cooling jacket, which may therefore undergo cavitation. This opens the possibility to design sono-reactors in which the working liquid is insulated from the sonotrode by a solid wall, which constitutes an interesting feature for electrochemical reactions, where electrical currents leaking through the metallic sonotrode should be avoided [9].

Besides, it has been shown that, exciting the sono-reactor near a resonance frequency may present two advantages. The first one lies simply in the large amplitude of the acoustic pressures obtained. The second is the possible localization of pressure antinode far from the emitter, which could avoid the well-known issue of cavitation-induced erosion of the sonotrode. This latter feature may however disappears for too strong attenuation.

The concepts of acoustic energy, intensity, active and dissipated powers have been clarified on a rigorous development, and illustrated by simulation. The key points are that, disregarding the acoustic energy transmitted to the surrounding air by boundaries, the active power is nothing else than the dissipated power in the liquid, averaged over one period. This was checked by simulation and represents indeed a

good test to check the validity of the numerical results. Besides it was shown that the approximation of plane traveling wave, commonly used in order to link the amplitude of the source to the active power, does not make sense.

Finally, a slight variation of the liquid properties shifts noticeably the resonance peaks, which demonstrates the interest of using a self-adjusting generator.

Linear acoustics therefore yields qualitatively interesting results in studying and designing sonoreactors, provided that the vibrations of the solid are accounted for. The main unknown remains the attenuation factor, strongly linked to the bubble repartition in the liquid, which in turn depends on the shape of the acoustic field [21]. Coupling both phenomena in a FEM model including the main physics of cavitation remains to be done, and constitutes a challenge for further studies.

Appendix A. Equations of energy conservation

A.1. *Theorem of kinetic energy*

For any mechanical system, the theorem of kinetic energy states that

$$\frac{dK}{dt} = \mathcal{P}_{\text{ext}} + \mathcal{P}_{\text{int}}, \tag{A.1}$$

where $\mathcal{P}_{\text{ext}}$ and $\mathcal{P}_{\text{int}}$ are the powers of external and internal forces respectively. In the case of an arbitrary volume V of fluid in motion, this equation reads

$$\frac{d}{dt}\iiint_V \frac{1}{2}\rho_l \mathbf{v}^2 \,\mathrm{d}V = \underbrace{\iint_S -p\mathbf{v}\mathbf{n}\,\mathrm{d}S}_{\substack{\text{Power of external}\\ \text{pressure forces}}} + \underbrace{\iiint_V p\boldsymbol{\nabla}.\mathbf{v}\,\mathrm{d}V}_{\substack{\text{Power of internal}\\ \text{pressure forces}}} + \underbrace{\iiint_V -\Pi_{\text{diss}}\,\mathrm{d}V}_{\substack{\text{Power of internal}\\ \text{dissipative forces}}}, \tag{A.2}$$

where $\Pi_{\text{diss}} > 0$ is the dissipation function. In the case of acoustic waves, using the mass conservation equation Eq. (1) to express $\boldsymbol{\nabla}.\mathbf{v}$ in the third integral, we obtain

$$\begin{aligned}\frac{d}{dt}\iiint_V \left(\frac{1}{2}\rho_l \mathbf{v}^2 + \frac{1}{2}\frac{p^2}{\rho_l c_l^2}\right)\mathrm{d}V = \\ \iint_S -p\mathbf{v}\mathbf{n}\,\mathrm{d}S + \iiint_V -\Pi_{\text{diss}}\,\mathrm{d}V,\end{aligned} \tag{A.3}$$

which is equation (19), in the case of non-dissipative waves ($\Pi_{\text{diss}} = 0$).

If mono-harmonic dissipative waves are assumed, the above equation can be averaged over one period, to yield:

$$\iint_S \frac{1}{2}\Re(P\mathbf{V}^*).\mathbf{n}\,\mathrm{d}S = \iiint_V -\langle\Pi_{\text{diss}}\rangle\,\mathrm{d}V. \tag{A.4}$$

The dissipated mechanical energy Π_{diss} can be deduced from the knowledge of the attenuation coefficient α (see Eq. (27)). To see that, we start from Eqs. (5), (6) assuming a complex wave number:

$$i\frac{\Re(k^2)}{\rho_l\omega}P + \boldsymbol{\nabla}.\mathbf{V} = \frac{\Im(k^2)}{\rho_l\omega}P, \tag{A.5}$$

$$i\omega\rho_l\mathbf{V} = -\boldsymbol{\nabla}P, \tag{A.6}$$

where $\Im$ denotes the imaginary part of a complex number. Multiplying the first by P^*, the transpose of the second by $\mathbf{V}$, summing, and taking the real part, we obtain:

$$\frac{1}{2}\nabla.\Re(P\mathbf{V}^*) = \frac{\Im(k^2)}{2\rho_l\omega}|P|^2. \tag{A.7}$$

Integrating on a volume V and using the divergence theorem:

$$\iint_S \frac{1}{2}\Re(P\mathbf{V}^*).\mathbf{n}\,\mathrm{d}S = \iiint_V \frac{\Im(k^2)}{2\rho_l\omega}|P|^2\,\mathrm{d}V. \tag{A.8}$$

Identifying this equation with equation (A.4), the average dissipated power density is therefore seen to read

$$\langle\Pi_{\text{diss}}\rangle = -\frac{\Im(k^2)}{2\rho_l\omega}|P|^2. \tag{A.9}$$

Further using the definition of the attenuation coefficient (27), the latter expression can be written as

$$\langle\Pi_{\text{diss}}\rangle = \frac{\alpha k_r}{\rho_l\omega}|P|^2, \tag{A.10}$$

and is clearly positive. Replacing k_r by ω/c_l, the dissipated power density finally becomes

$$\langle\Pi_{\text{diss}}\rangle = \alpha\frac{|P|^2}{\rho_l c_l}. \tag{A.11}$$

The quantity $|P|^2/(\rho_l c_l)$ is sometimes erroneously termed as "intensity". We emphasize that this is true

only for plane traveling wave, but is definitely not in other cases. Expression (A.11) remains however valid, and allows to estimate $|P|$ by measuring Π_{diss}, generally equating the latter to $\rho_l C_p (dT/dt)_0$.

Acknowledgements

The authors thank Generalidad Valenciana (Spain) for its financial support under Projects AINV07/044 and AE/07/079 and also to COST D32 for the framework. JK gratefully thanks the Ministry of Education, Youth and Sports (MSMT) of the Czech Republic for financial support (grant number 1P05OC074).

References

[1] T. J. Leighton, The acoustic bubble, Academic Press, 1994.

[2] L. A. Crum, T. J. Mason, J. L. Reisse, K. S. Suslick (Eds.), Sonochemistry and Sonoluminescence, Kluwer Academic, Dordrecht, 1999, proceedings of the NATO Advanced Study Institute on Sonoluminescence and Sonoluminescence, Leavenworth, Washington, USA, 18-29 August 1997.

[3] K. S. Suslick, Ultrasound. Its chemical, Physical and Biological effects., VCH Publishers, New-York, 1988.

[4] R. Mettin, Bubble structures in acoustic cavitation, in: A. A. Doinikov (Ed.), Bubble and Particle Dynamics in Acoustic Fields: Modern Trends and Applications, Research Signpost, Kerala (India), 2005, pp. 1–36.

[5] L. van Wijngaarden, On the equations of motion for mixtures of liquid and gas bubbles, J. Fluid Mech. 33 (3) (1968) 465–474.

[6] K. W. Commander, A. Prosperetti, Linear pressure waves in bubbly liquids: comparison between theory and experiments, J. Acoust. Soc. Am. 85 (2) (1989) 732–746.

[7] R. E. Caflish, M. J. Miksis, G. C. Papanicolaou, L. Ting, Effective equations for wave propagation in bubbly liquids, J. Fluid Mech. 153 (1985) 259–273.

[8] V. Sáez, A. Frías-Ferrer, J. Iniesta, J. González-García, A. Aldaz, E. Riera, Characterization of a 20 khz sonoreactor. part i: analysis of mechanical effects by classical and numerical methods., Ultrason. Sonochem. 12 (2005) 59–65.

[9] J. Klíma, A. Frías-Ferrer, J. González-García, J. Ludvík, V. Sáez, J. Iniesta, Optimisation of 20 khz sonoreactor geometry on the basis of numerical simulation of local ultrasonic intensity and qualitative comparison with experimental results., Ultrason. Sonochem. 14 (2007) 19–28.

[10] K. Yasui, T. Kozuka, T. Tuziuti, A. Towata, Y. Iida, J. King, P. Macey, Fem calculation of an acoustic field in a sonochemical reactor, Ultrason. Sonochem. 14 (2007) 605–614.

[11] M. Romdhane, C. Gourdon, G. Casamatta, Thermoelectric sensor for ultrasonic intensity measurement, Ultrasonics 33 (2) (1995) 139–146.

[12] P. M. Morse, K. U. Ingard, Theoretical acoustics, McGraw-Hill, 1968.

[13] J. C. Devin, Survey of thermal, radiation and viscous damping of pulsating air bubbles in water, J. Acoust. Soc. Am. 31 (12) (1959) 1654–1667.

[14] A. Prosperetti, Thermal effects and damping mechanisms in the forced radial oscillations of gas bubbles in liquids., J. Acoust. Soc. Am. 61 (1) (1977) 17–27.

[15] L. A. Crum, A. Prosperetti, Nonlinear oscillations of gas bubbles in liquids: an interpretation of some experimental results., J. Acoust. Soc. Am. 73 (1) (1983) 121–127.

[16] L. A. Crum, The polytropic exponent of gas contained within air bubbles pulsating in a liquid, J. Acoust. Soc. Am. 73 (1) (1983) 116–120.

[17] S. Dähnke, K. M. Swamy, F. J. Keil, Modeling of three-dimensional pressure fields in sonochemical reactors with an inhomogeneous density distribution of cavitation bubbles. comparison of theoretical and experimental results, Ultrason. Sonochem. 6 (1999) 31–41.

[18] G. Servant, J. P. Caltagirone, A. Grard, J. L. Laborde, A. Hita, Numerical simulation of cavitation bubble dynamics induced by ultrasound waves in a high frequency reactor, Ultrason. Sonochem. 7 (2000) 217–227.

[19] G. Servant, J. L. Laborde, A. Hita, J. P. Caltagirone, A. Grard, On the interaction between ultrasound waves and bubble clouds in mono- and dual-frequency sonoreactors, Ultrason. Sonochem. 10 (6) (2003) 347–355.

[20] W. Lauterborn, T. Kurz, R. Mettin, C. D. Ohl, Experimental and theoretical bubble dynamics, Adv. Chem. Physics 110 (1999) 295–380.

[21] R. Mettin, P. Koch, W. Lauterborn, D. Krefting, Modeling acoustic cavitation with bubble redistribution, in: Sixth International Symposium on Cavitation - CAV2006 (paper 75), Wageningen (The Netherlands), 2006, pp. 125–129.